

Cite this: *Chem. Commun.*, 2011, **47**, 6677–6679

www.rsc.org/chemcomm

COMMUNICATION

Highly ordered acid functionalized SBA-15: a novel organocatalyst for the preparation of xanthenes†

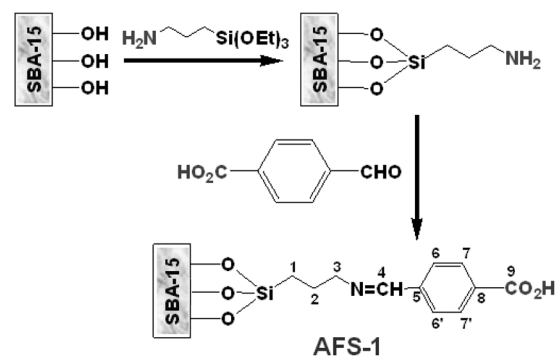
Mahasweta Nandi,^{ab} John Mondal,^a Krishanu Sarkar,^a Yusuke Yamauchi^c and Asim Bhaumik^{*a}

Received 21st February 2011, Accepted 8th April 2011

DOI: 10.1039/c1cc11007a

Post-synthesis modification of SBA-15 has been carried out to design highly ordered acid functionalized hybrid mesoporous organosilica, AFS-1. This material has been used as an efficient heterogeneous organocatalyst for the syntheses of xanthenes under mild conditions in the absence of any other metal co-catalyst.

Xanthenes are a class of compounds which are hugely recognized in the field of medicine and organic chemistry due to their antiviral,¹ antibacterial² and anti-inflammatory³ activities. They are the source of a class of brilliant fluorescent dyes⁴ and are used extensively in laser technology⁵ and pH sensitive fluorescent materials.⁶ Several methods for the syntheses of substituted xanthene *via* reaction of 2-naphthol with aryl aldehydes under strongly acidic conditions are reported in the literature.⁷ Most of these syntheses either involve the use of metal containing catalysts⁸ or suffer from serious drawbacks like long reaction time, low yield, vigorous reaction conditions and so on.⁹ Owing to the toxic effects and deactivation associated with metal-leaching during the reaction, increasing interests are being paid for the development of organocatalysts devoid of metal ions.¹⁰ Transformations involving an organocatalyst can be considered as a green process but they are mostly homogeneous in nature.¹¹ Thus catalyst recovery and its reuse is an important drawback associated with an organocatalytic reaction. To avoid these problems heterogeneous organocatalysts can be very promising, particularly those based on mesoporous silica due to their exceptional surface area, tuneable nano-scale pores, and exciting host-guest chemistry.¹² Thus the syntheses of organically modified mesoporous silica with new framework structures are highly desirable. In this communication, we report a new surface $-\text{CO}_2\text{H}$ group functionalized mesoporous silica, with a 2D-hexagonal mesoporous structure



Scheme 1 Schematic diagram for acid functionalization of SBA-15.

via consecutive surface functionalization with 3-aminopropyl triethoxysilane (3-APTES) followed by the condensation of the surface $-\text{NH}_2$ groups with the aldehyde group of 4-formylbenzoic acid (Scheme 1). Previously $-\text{CO}_2\text{H}$ and $-\text{SO}_3\text{H}$ functionalized mesoporous SBA-15 has been reported by co-condensation¹³ and post-synthesis grafting¹⁴ techniques, respectively. However, incorporation of the $-\text{CO}_2\text{H}$ group into a mesoporous silica framework by condensation between an aldehyde and a primary amine has not been studied so far. Increasing importance of metal-free catalysis, on the other hand, motivated us to use this organically modified acid functionalized mesoporous silica (AFS-1) as a catalyst for the synthesis of benzoxanthene from a mixture of aromatic aldehyde and 2-naphthol. To the best of our knowledge, organocatalysis promoted by a $-\text{CO}_2\text{H}$ functionalized mesoporous silica for the synthesis of xanthene has not been explored so far.

Mesoporous silica, SBA-15, has been synthesized following the reported procedure.¹⁵ It is modified with 3-APTES by stirring 0.1 g of SBA-15 with 0.18 g (0.813 mmol) of the former in chloroform at 298 K for 12 h under a N_2 atmosphere. The resulting white solid is filtered, washed repeatedly with chloroform and dichloromethane (DCM), and finally dried in air. This 3-APTES functionalized SBA-15 is refluxed with 0.15 g (1 mmol) of 4-formylbenzoic acid dissolved in methanol (20 ml) for 6 h at 333 K and the final product is collected by filtration, repeatedly washed with hot methanol until all the unreacted carboxylic acid is removed and finally dried in a vacuum desiccator. In a typical catalytic cycle, a mixture of 2 mmol 2-naphthol and 1 mmol aromatic aldehyde is stirred with 20 mg of AFS-1 in the presence of 5 ml dry DCM at 298 K for the

^a Department of Materials Science, Indian Association for the Cultivation of Science, Jadavpur, Kolkata-700 032, India. E-mail: msab@iacs.res.in; Fax: +91-33-2473-2805; Tel: +91-33-2473-4971

^b Integrated Science Education and Research Centre, Siksha Bhavana, Visva-Bharati, Santiniketan-731235, India

^c World Premier International (WPI) Research Center for Materials Nanoarchitectonics (MANA), National Institute for Materials Science (NIMS), Namiki 1-1, Tsukuba, Ibaraki 305-0044, Japan

† Electronic supplementary information (ESI) available: TEM, TG-DTA, solid state ^{13}C MAS NMR and recycling tests of AFS-1 and ^1H and ^{13}C NMR of the reaction products. See DOI: 10.1039/c1cc11007a

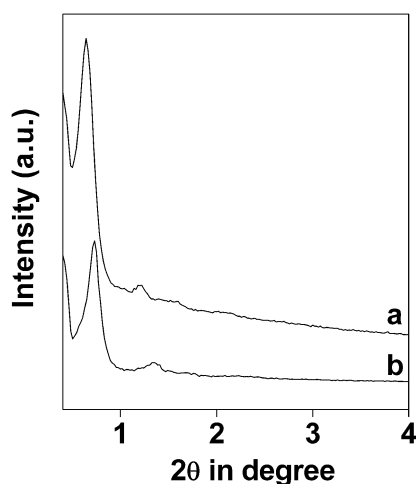


Fig. 1 Low angle XRD pattern of SBA-15 (a) and AFS-1 (b).

desired time. After completion of the reaction, the catalyst is filtered from the reaction mixture, washed thoroughly with DCM and the filtrate is evaporated to dryness under reduced pressure. The crude solid product obtained is crystallized from ethanol. The recovered catalyst is washed with ether and dried at 353 K for 2 h prior to use for the next cycle.

Quantitative estimation shows that the loading of 3-APTES in 3-APTES-SBA-15 and 4-formylbenzoic acid in AFS-1 are $0.0075 \text{ mol g}^{-1}$ and $0.0045 \text{ mol g}^{-1}$ respectively. These values can be correlated to *ca.* 82% conversion of the amino groups to corresponding Schiff-base in AFS-1. The small-angle powder X-ray diffraction (PXRD) patterns of mesoporous SBA-15 and AFS-1 are shown in Fig. 1. For SBA-15 (Fig. 1a) four well-resolved diffraction peaks in the 2θ region of 0.6–2.07 can be observed, which can be indexed to the 100, 110, 200 and 210 reflections¹⁶ corresponding to a two-dimensional hexagonal mesostructure. When the silica framework is functionalized with the acid groups a decrease in the intensity of the peaks is observed, however the 2D-hexagonal ordering is retained. This decrease in the peak intensities is attributed to the lowering of local order, *viz.* variations in the wall thickness or reduction of scattering contrast between the channel wall of the silicate framework.¹⁷ The TEM images (ESI†, Fig. S1) of mesoporous SBA-15 and acid functionalized material AFS-1 show uniform and long range ordering of large mesopores throughout the respective specimens. The corresponding FFT diffractogram (inset of Fig. S1a, ESI†) further suggests the presence of hexagonally arranged pores.¹⁸

Nitrogen-sorption studies carried out on the calcined mesoporous SBA-15 and AFS-1 at 77 K are shown in Fig. 2. Both the samples show type-IV adsorption-desorption isotherms with a very large H_2 type hysteresis loop in the 0.5 to 0.8 P/P_0 range. The sharpness of the adsorption step in these isotherms suggest the relative order in mesopore size and the characteristic hysteresis loop account for the large-tubular pores of SBA-15.¹⁸ The surface area of SBA-15 (Fig. 2a) is $610 \text{ m}^2 \text{ g}^{-1}$ and that for AFS-1 is reduced to $250 \text{ m}^2 \text{ g}^{-1}$ (Fig. 2b). The values of P/P_0 near the inflection point are closely related to the pore-widths which lie in the mesopore range and the sharpness of these steps indicates the uniform size distribution of the mesopores.¹⁸ Pore size distribution of both the samples estimated employing the

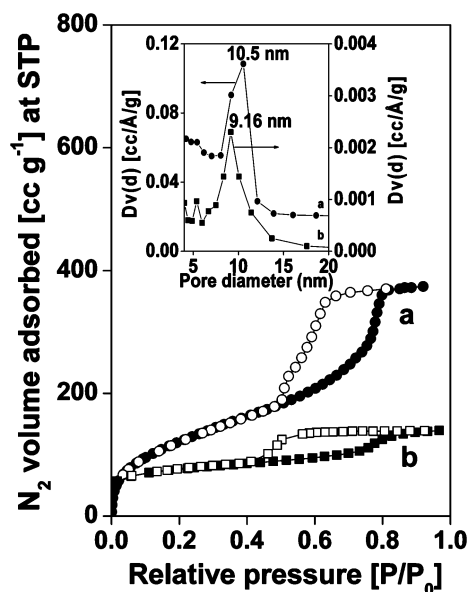


Fig. 2 Nitrogen adsorption-desorption isotherm of SBA-15 (a) and AFS-1 (b). Inset: pore size distribution using the BJH method.

Barett-Joyner-Halenda (BJH) method is shown in the inset of Fig. 2. Estimated pore width for SBA-15 is 10.5 nm whereas for AFS-1 the pore size is reduced to 9.16 nm. These data are in good agreement with the pore widths depicted by the TEM image analysis and XRD studies.

^{13}C and ^{29}Si MAS NMR experiments often provide useful information regarding the chemical environment and the presence of an organic functional group in the hybrid frameworks. The ^{13}C CP MAS NMR spectrum (ESI†, Fig. S2) for AFS-1 exhibits three strong signals at 9.1, 21.8 and 43.5 ppm. Sharp peaks could be assigned to the aliphatic propyl group attached with Si, C1, C2 and C3 respectively (Scheme 1). Four other broad signals with maximums at 62.8, 130.6, 140.1 and 164.2 could be attributed to imine-C, benzene rings and $-\text{CO}_2\text{H}$ groups, respectively. This result indicates that the functional group bearing the acid moiety is covalently grafted inside the pore walls of AFS-1. On the other hand the ^{29}Si MAS NMR spectra of AFS-1 (Fig. 3) show two broad peaks with chemical

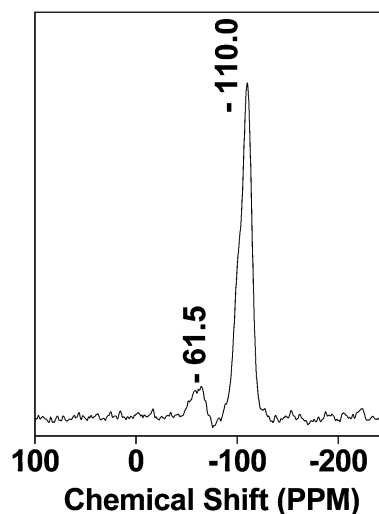
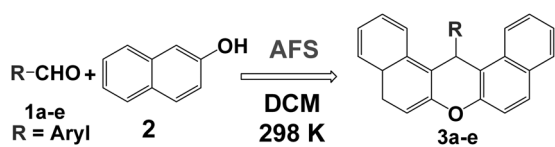


Fig. 3 ^{29}Si MAS NMR spectra of AFS-1.



Scheme 2 General protocol for xanthene synthesis over **AFS-1**.

shifts at -61.5 and -110.0 ppm, which could be attributed to the T^3 ($(OH)(OSi)_3Si-R$) and Q^4 ($Si(OSi)_4$) species, respectively.¹⁹ Presence of high concentration of Q^4 and T^3 species in the NMR spectrum of **AFS-1** suggested a considerably defect-less cross-linked network in the material. Thermal analysis of SBA-15, 3-APTES-functionalized SBA-15 and **AFS-1** (ESI†, Fig. S3 and S4) has been carried out to compare the stability of the catalyst, which is an important issue associated with a heterogeneous catalytic system. For the synthesis of xanthene, we have carried out the reactions at room temperature, but **AFS-1** is found to have sufficient thermal stability to carry out other organocatalytic reactions, which can occur at higher temperature. The total weight loss for the material upto 773 K is found to be 16% which takes place in two steps. The first step is associated with the removal of physisorbed water, whereas the second step involving combustion of the organic functionality present in the organosilane framework starts above 473 K.

AFS-1 is investigated for its catalytic activity for the preparation of xanthene in the absence of any other metal co-catalyst. It is found that condensation between aromatic aldehydes (**1a-e**) and 2-naphthol (**2**) at room temperature (Scheme 2, Table 1) produces 14-aryl-14H-dibenzo [a,j] xanthenes in good yields over our **AFS-1** material. The products are characterized by 1H and ^{13}C NMR spectroscopy and the data are given in ESI.†

The heterogeneous nature of the catalyst has been confirmed by performing *in situ* filtration experiment for the reaction between 4-nitrobenzaldehyde and 2-naphthol, as a representative case. The catalyst has been separated from the reaction mixture by filtration after 1 h (30% conversion). The reaction was continued with the filtrate for another 4 h but no further conversion took place. To test the catalytic efficiency of **AFS-1**, the recovered catalyst was successively used in six repeating cycles (ESI†, Fig. S5). No appreciable loss of reactivity was observed. After 4 h reaction time in each of the cycles, above 75% conversion took place and the same catalyst can be used repetitively to give very good overall turnover numbers (TON, Table 1). Thus we see that **AFS-1** acts as a highly efficient and recyclable organocatalyst for the synthesis of xanthenes.

Table 1 Synthesis of 14-aryl-14H-dibenzo [a,j] xanthenes

Entry	Aldehyde	Time/h	Yield (%)	Product	TON
1		4.0	82	3a	9.1
2		5.0	80	3b	8.9
3		4.5	75	3c	8.3
4		4.0	75	3d	8.3
5		5.0	78	3e	8.7

In conclusion, we have shown that new functionalized mesoporous material **AFS-1** can be used as an extremely stable and reusable catalyst for the preparation of xanthenes from a mixture of β -naphthol and aromatic aldehyde. This reaction proceeds smoothly at room temperature in the absence of any other metal-containing species and the catalytic efficiency is restored in repeated reaction cycles. This is the first example of organocatalysis promoted by a $-COOH$ functionalized mesoporous silica for the synthesis of xanthenes and it opens up a new direction for the development of catalysts devoid of toxic metals and their further applications in various organic transformations.

JM wishes to thank CSIR, New Delhi, for Senior Research Fellowship.

Notes and references

- R. F. Schinazi and R. A. Floyd, *PCT Int. Appl.*, 1990, WO 9013296 A1 19901115.
- (a) E. Krumkalns, *U.S.*, US 3335148 19670808, 1967; (b) W. Hong, L. Lei, Z. Shiyun, L. Yahong and C. Weimin, *Curr. Microbiol.*, 2006, **52**, 1–5.
- H. N. Hafez, M. I. Hegab, I. S. Ahmed-Farag and A. B. A. El-Gazzar, *Bioorg. Med. Chem. Lett.*, 2008, **18**, 4538–4543.
- F. Mao, W.-Y. Leung and C.-Y. Cheung, *U.S. Pat. Appl. Publ.*, 2010, US 20100197030 A1 20100805.
- M. Bass, T. F. Deutsch and M. J. Weber, *Appl. Phys. Lett.*, 1968, **13**, 120–124.
- (a) E. Kuwana and E. M. Seveck-Muraca, *Anal. Chem.*, 2003, **75**, 4325–4329; (b) K. P. McNamara, T. Nguyen, G. Dumitrascu, J. Ji, N. Rosenzweig and Z. Rosenzweig, *Anal. Chem.*, 2001, **73**, 3240–3246.
- (a) Y.-H. Liu, X.-Y. Tao, L.-Q. Lei and Z.-H. Zhang, *Synth. Commun.*, 2009, **39**, 580–589; (b) X. Huang and T. X. Zhang, *J. Org. Chem.*, 2010, **75**, 506–509.
- M. Dabiri, M. Baghbanzadeh, M. S. Nikcheh and E. Arzroomchilar, *Bioorg. Med. Chem. Lett.*, 2008, **18**, 436–438.
- B. Das, B. Ravikanth, R. Ramu, K. Laxminarayana and B. V. Rao, *J. Mol. Catal. A: Chem.*, 2006, **255**, 74–77.
- S. Bertelsen and K. A. Jorgensen, *Chem. Soc. Rev.*, 2009, **38**, 2178–2189.
- (a) J. Franzen and A. Fisher, *Angew. Chem., Int. Ed.*, 2009, **48**, 787–791; (b) B. Tan, X. F. Zeng, Y. P. Lu, P. J. Chua and G. F. Zhong, *Org. Lett.*, 2009, **11**, 1927–1930; (c) N. Bravo, I. Mon, X. Companyo, A. N. Alba, A. Moyano and R. Rios, *Tetrahedron Lett.*, 2009, **50**, 6624–6626; (d) S. Piovesana, D. M. S. Schietroma, L. G. Tulli, M. R. Monaco and M. Bella, *Chem. Commun.*, 2010, **46**, 5160–5162.
- (a) M. E. Davis, *Nature*, 2002, **417**, 813–821; (b) R. K. Zeidan, S.-J. Hwang and M. E. Davis, *Angew. Chem., Int. Ed.*, 2006, **45**, 6332–6335; (c) E. L. Margelefsky, R. K. Zeidan and M. E. Davis, *Chem. Soc. Rev.*, 2008, **37**, 1118–1126; (d) S. A. El-Safty, M. Mekawy, A. Yamaguchi, A. Shahat, K. Ogawa and N. Teramae, *Chem. Commun.*, 2010, **46**, 3917–3919.
- (a) S. Fiorilli, B. Onida, B. Bonelli and E. Garrone, *J. Phys. Chem. B*, 2005, **109**, 16725–16729; (b) J. S. Gao, J. Liu, S. Y. Bai, P. Y. Wang, H. Zhong, Q. H. Yang and C. Li, *J. Mater. Chem.*, 2009, **19**, 8580–8588.
- M. A. Naik, D. Sachdev and A. Dubey, *Catal. Commun.*, 2010, **11**, 1148–1153.
- S. K. Das, M. K. Bhunia and A. Bhaumik, *J. Solid State Chem.*, 2010, **183**, 1326–1333.
- C. T. Kresge, M. E. Leonowicz, W. J. Roth, J. C. Vartuli and J. S. Beck, *Nature*, 1992, **359**, 710–712.
- M. H. Lim and A. Stein, *Chem. Mater.*, 1999, **11**, 3285–3295.
- D. Y. Zhao, Q. S. Huo, J. L. Feng, B. F. Chmelka and G. D. Stucky, *J. Am. Chem. Soc.*, 1998, **120**, 6024–6036.
- (a) J. Liu, Q. H. Yang, M. P. Kapoor, N. Satoyama, S. Inagaki, J. Yang and L. Zhang, *J. Phys. Chem. B*, 2005, **109**, 12250–12256; (b) B. D. Hatton, K. Kandskron, W. Whitnall, D. D. Perovic and G. A. Ozin, *Adv. Funct. Mater.*, 2005, **15**, 823–829; (c) U. Diaz, T. Garcia, A. Vely and A. Corma, *J. Mater. Chem.*, 2009, **19**, 5970–5979; (d) A. Modak, J. Mondal, V. K. Aswal and A. Bhaumik, *J. Mater. Chem.*, 2010, **20**, 8099–8106.